

Photovoltaic Properties of CdSe Quantum Dot Sensitized Inverse Opal TiO₂ Solar Cells: The Effect of TiCl₄ Post Treatment

Motoki Hironaka¹, Taro Toyoda¹, Kanae Hori¹, Yuhei Ogomi², Shuzi Hayase², Qing Shen^{1*}

¹Department of Engineering Science, The University of Electro-Communications, Chofu, Japan

²Graduate School of Life Science and Systems Engineering, Kyushu Institute of Technology, Kitakyushu, Japan

Email: *shen@pc.uec.ac.jp

How to cite this paper: Hironaka, M., Toyoda, T., Hori, K., Ogomi, Y., Hayase, S. and Shen, Q. (2017) Photovoltaic Properties of CdSe Quantum Dot Sensitized Inverse Opal TiO₂ Solar Cells: The Effect of TiCl₄ Post Treatment. *Journal of Modern Physics*, 8, 522-530.

<https://doi.org/10.4236/jmp.2017.84034>

Received: February 14, 2017

Accepted: March 14, 2017

Published: March 17, 2017

Copyright © 2017 by authors and Scientific Research Publishing Inc. This work is licensed under the Creative Commons Attribution International License (CC BY 4.0).

<http://creativecommons.org/licenses/by/4.0/>



Open Access

Abstract

Recently, semiconductor quantum dot (QD) sensitized solar cells (QDSSCs) are expected to achieve higher conversion efficiency because of the large light absorption coefficient and multiple exciton generation in QDs. The morphology of TiO₂ electrode is one of the most important factors in QDSSCs. Inverse opal (IO) TiO₂ electrode, which has periodic mesoporous structure, is useful for QDSSCs because of better penetration of electrolyte than conventional nanoparticulate TiO₂ electrode. In addition, the ordered three dimensional structure of IO-TiO₂ would be better for electron transport. We have found that open circuit voltage V_{oc} of QDSSCs with IO-TiO₂ electrodes was much higher (0.2 V) than that with nanoparticulate TiO₂ electrodes. But short circuit current density J_{sc} was lower in the case of IO-TiO₂ electrodes because of the smaller surface area of IO-TiO₂. In this study, for increasing surface area of IO-TiO₂, we applied TiCl₄ post treatment on IO-TiO₂ and investigated the effect of the post treatment on photovoltaic properties of CdSe QD sensitized IO-TiO₂ solar cells. It was found that J_{sc} could be enhanced due to TiCl₄ post treatment, but decreased again for more than one cycle treatment, which indicates excess post treatment may lead to worse penetration of electrolyte. Our results indicate that the appropriate post treatment can improve the energy conversion efficiency of the QDSSCs.

Keywords

Quantum Dot Sensitized Solar Cells, Inverse Opal Structure, TiCl₄ Post Treatment, Morphology of the TiO₂ Electrode

1. Introduction

One of the potential candidates for next generation solar cells is dye sensitized

solar cells (DSSCs), due to their high energy conversion efficiency exceeding 10% [1]. However, the photovoltaic performance of DSSCs is needed to be further improved in order to replace conventional Si-based solar cell in practical applications. From the viewpoint of sensitizers, semiconductor quantum dot (QD) sensitized solar cells (QDSSCs) have been the focus of much attention as candidates for replacing the sensitizer dyes in DSSCs, due to their specific advantages in solar cell applications [2] [3] [4]. For example, the QDs show tunable band gap by controlling their sizes, so that the absorption spectra of the QDs can be tuned to match the spectral distribution of sunlight. Moreover, the QDs have large extinction coefficients and a potential to generate multiple electron-hole pairs with one single photon absorption [5].

On the other hand, the morphology of the TiO_2 electrode is one of the most important factors in QDSSCs. However, the normal TiO_2 electrode has a disordered assembly of nanoparticle structure, causing the poor penetration of electrolyte. In our previous study, we have demonstrated that inverse opal (IO) structure TiO_2 electrode, which has ordered periodic mesoporous structure, is useful for QDSSCs because of better penetration of electrolyte than conventional nanoparticulate structure [6]. Moreover, this structure has the possibility of enhancing the light harvesting efficiency, due to the slow light effect by photonic band gap which depends on the filling fraction of TiO_2 in the IO structure [7].

We have proposed the use of IO- TiO_2 solar cell sensitized with CdSe QDs by chemical bath deposition (CBD) method [6]. In addition, the CdSe QDs were coated with ZnS for surface passivation. We have found that open circuit voltage V_{oc} of QDSSCs with IO- TiO_2 electrodes were much higher (about 0.7 V) than that with nanoparticulate TiO_2 electrodes (about 0.5 V). But short circuit current density J_{sc} was lower in the case of IO- TiO_2 electrodes because of the smaller surface area of the IO- TiO_2 [6]. In this study, to increase surface area of IO- TiO_2 , we have applied TiCl_4 post treatment on IO- TiO_2 and investigated the effect of the post treatment on photovoltaic properties of CdSe QD sensitized IO- TiO_2 solar cells. We found that the photovoltaic performance changed systematically by increasing the TiCl_4 post treatment cycles on IO- TiO_2 .

2. Experiment

IO- TiO_2 electrodes were prepared on fluorine-doped tin oxide (FTO) conducting glass ($10 \Omega/\text{sq}$) by the sol - gel method [8]. Substrates were cleaned ultrasonically with acetone and methanol. Monodisperse polystyrene latex (PSL) suspensions (304 nm in diameter) were sonicated for 30 min to split the aggregated particles. The synthetic opal templates were assembled by immersing FTO substrate vertically in 0.125 wt% PSL suspension and evaporating the solvent in an oven at 40°C until the solvent completely disappeared, leaving behind a colloidal PSL film on the substrate. Then TiO_2 was brought into the void of the template by the following method. The substrate was immersed into TiO_2 precursor solution with mixtures of absolute ethanol, hydrochloric acid, tetrabutyl titanate, and deionized water for 10 min [8]. The substrate was subsequently heated at 450°C

for 3 h in air with a heating rate of 1°C/min to calcine the template and anneal the TiO₂. For the post treatment on the surface of IO-TiO₂, the substrate was immersed into 50 mM TiCl₄ solution at 70°C for 1 h and subsequently heated at 450°C. The processes were repeated several times (1, 2, 3 cycles). After the TiCl₄ post treatment, CdSe QDs were adsorbed on IO-TiO₂ electrode at 10°C for 9 h using a chemical bath deposition (CBD) method [6]. The deposition solution was prepared by adding 0.7 M sodium nitrilotriacetate [N(CH₂COONa)₃ or simply as NTA] to 0.5 M CdSO₄. Then 0.2 M sodium selenosulfate (Na₂SeSO₃) in excess Na₂SO₃, prepared by stirring 0.2 M Se with 0.5 M Na₂SO₃ at 70°C for 4 h, was added, giving a final composition of 80 mM CdSO₄, 80 mM Na₂SeSO₃ (which includes 0.12 M free Na₂SO₃), and 120 mM NTA. During the deposition, the TiO₂ electrodes were placed in the solution at 10°C in the dark for 9 h. After CdSe QD adsorption, the electrode was coated with ZnS by twice dipping alternately into 0.1 M Zn(CH₃COO)₂ and Na₂S solution for 1 min [9]. The morphologies of samples were observed by scanning electron microscopy (SEM) and transmission electron microscopy (TEM). The optical absorption of TiO₂ electrodes with CdSe QDs were studied by using the photoacoustic (PA) technique. The PA method is a useful tool for opaque and scattered solid samples because the signal is directly proportional to the acoustic energy by heat generated through the optical absorption resulting from nonradiative processes [9]. **Figure 1** shows the schematic diagram of PA spectroscopy. The light source was a 300 W xenon short arc lamp. Monochromatic light through a monochromator was modulated with a mechanical chopper at frequency of 33 Hz. The PA spectra were normalized by using PA signals from a carbon black. The photocurrent density (J) versus photovoltage (V) characteristic measurements were performed in sandwich structure solar cells with using a CdSe QD sensitized electrode as the working electrode and Cu₂S as the counter electrode. The effective cell area was 0.25 cm², while the polysulfide electrolyte (1M Na₂S and 1M S solution) was used as redox couple [10]. The photovoltaic characteristics of the solar cells were measured using a solar simulator (Peccell technologies, Inc.) with 100 mW/cm² irradiation AM 1.5.

3. Results and Discussion

Figure 2 shows the typical SEM images of IO-TiO₂ without TiCl₄ post treatment (a), with one cycle TiCl₄ post treatment (b), with two cycles TiCl₄ post treatment

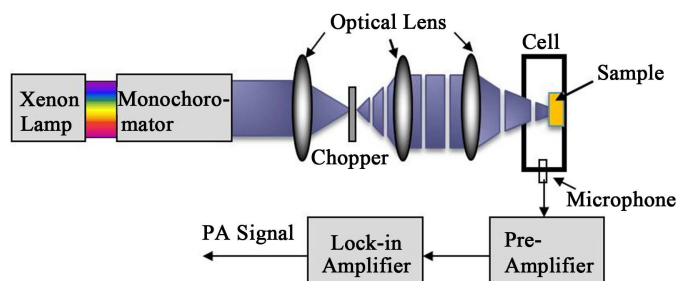


Figure 1. Schematic diagram of photoacoustic (PA) spectroscopy.

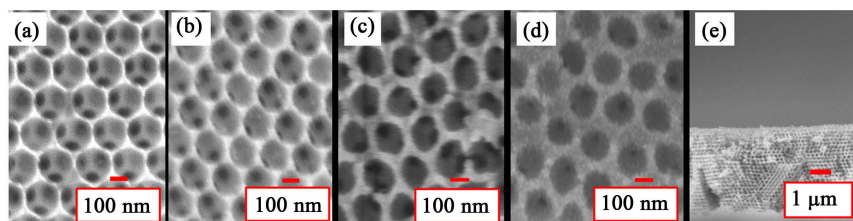


Figure 2. SEM images of the surfaces of IO-TiO₂ without TiCl₄ post treatment (a), with one cycle TiCl₄ post treatment (b), with two cycles TiCl₄ post treatment (c), with three cycles TiCl₄ post treatment (d) and cross section of IO-TiO₂ (e).

(c) and with three cycles TiCl₄ post treatment (d) and cross section of IO-TiO₂ (e). As shown in **Figure 2**, after the calcination of latex template, a honeycomb structure appears with an ordered hexagonal pattern of spherical pores that connect each sphere to its nearest neighbors. The diameter or center to center distance of the pores, referred to as the periodic lattice constant of IO-TiO₂, was determined to be ~230 nm (**Figure 2(a)**) which shows the shrinkage of the 304 nm diameter PSL particles. This structure consists of several layers connected to each other as shown in **Figure 2(a)** and **Figure 2(e)**. The wall of the IO-TiO₂ became thicker after the post treatment and increased as the post treatment cycle increased as shown in **Figures 2(a)-(d)**. The dependence of the thickness of the wall on post treatment cycle is shown in **Figure 3(a)**. The wall thickness increased from 17 nm to 47 nm after 3 cycle post treatment. **Figure 4** shows typical TEM images of IO-TiO₂ without TiCl₄ post treatment (a) and with three cycles post treatment (b). After TiCl₄ post treatment, TiO₂ adsorbed orderly along IO-TiO₂ surface were observed. The reflection spectrum of IO-TiO₂ using 304 nm PSL particles had a peak at 740 nm, indicating that IO-TiO₂ has a photonic crystal character. According to Bragg equation applied to the IO-TiO₂ (76% void), the peak value is in good agreement with the Bragg equation [11].

Figure 5 shows the typical SEM images of the surface of IO-TiO₂ after CdSe QD deposition, where the IO-TiO₂ was not post treated with TiCl₄ (a), and post treated with TiCl₄ once (b), twice (c) and three times (d). The CdSe were adsorbed orderly along IO-TiO₂ surface and the thickness of the wall became larger as the post treatment cycles increased. The dependence of the thickness of the wall of CdSe deposited IO-TiO₂ (IO-TiO₂/CdSe QDs) on post treatment cycle is shown in **Figure 3(b)**. **Figure 3(c)** shows the difference of the wall thickness between IO-TiO₂/CdSe QDs and IO-TiO₂ before CdSe deposition for each post treatment cycle. As shown in **Figure 3(c)**, the amount of the adsorbed CdSe QDs increased after the post treatment cycle increased. This is because of the surface area increased after the post treatment, which can also be observed from the TEM images.

Figure 6 shows the PA spectra of the IO-TiO₂/CdSe QD treated with and without TiCl₄ post treatment electrodes. The values of first excitation energies, E_1 , of the CdSe QDs for each sample are estimated from the optical shoulders in the PA spectra [10]. Relative to the band gap energy of 1.73 eV for bulk CdSe, blue shifts are observed for all samples due to the quantum confinement effect.

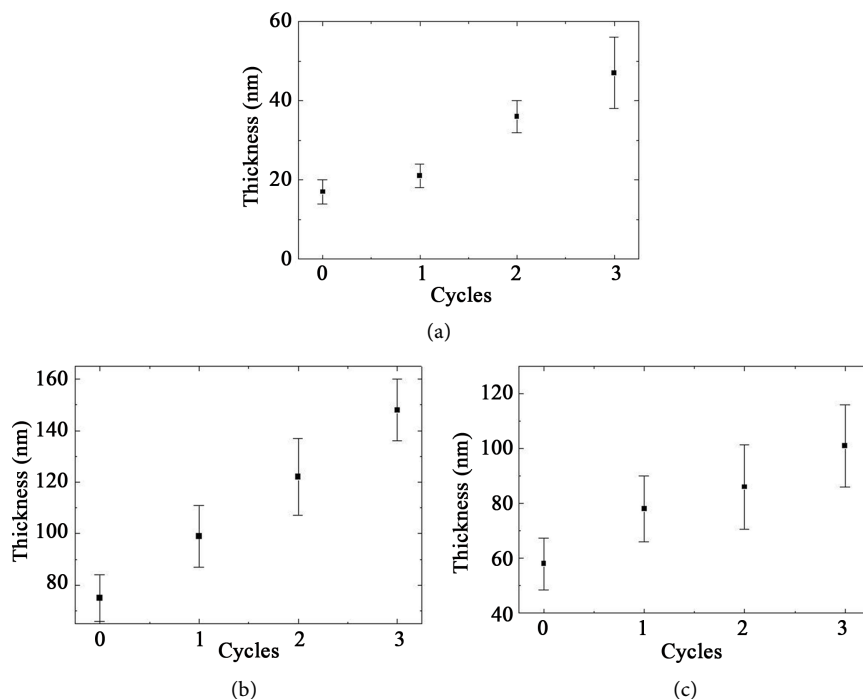


Figure 3. Dependence of the wall thickness of (a) the IO-TiO₂, (b) the IO-TiO₂/CdSe QDs and (c) the wall thickness difference between IO-TiO₂/CdSe QDs and IO-TiO₂ on the TiCl₄ post treatment cycles.

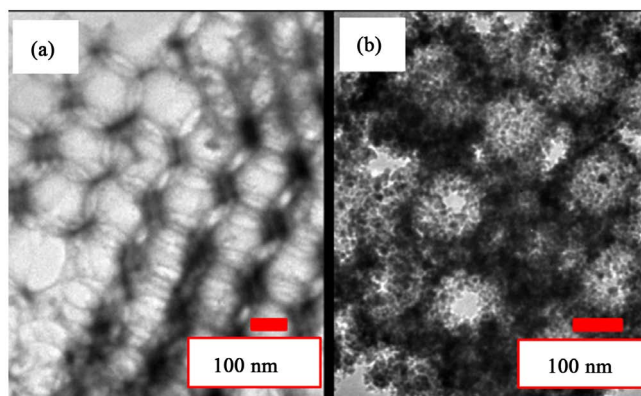


Figure 4. TEM images of the surfaces of IO-TiO₂ without TiCl₄ post treatment (a) and with three cycles TiCl₄ post treatment (b).

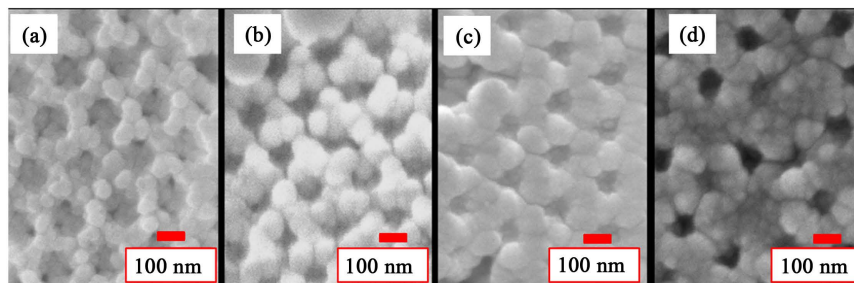


Figure 5. SEM images of the surfaces of CdSe deposited IO-TiO₂ without TiCl₄ post treatment (a), with one cycle TiCl₄ post treatment (b), with two cycles TiCl₄ post treatment (c), with three cycles TiCl₄ post treatment (d).

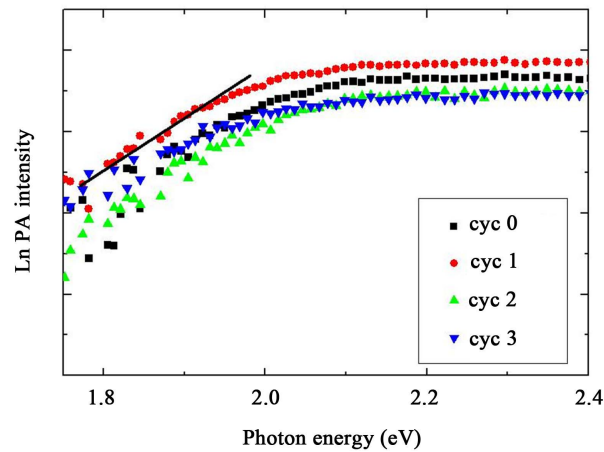


Figure 6. The PA spectra of the IO-TiO₂/CdSe QD electrodes treated without and with TiCl₄ post treatment for different cycles.

The average sizes of the CdSe QDs were about 6 nm calculated using the theory of effective mass approximation [9] [12]. Studies of the Urbach rule [13], which shows the low energy exponential tail depends on the photon energy, give information about disorders and impurities states. The dependence of the PA intensity on photon energy at the lower energy tail can be given by the following relationship

$$P = P_0 \exp\left[-\sigma \frac{(E_0 - h\nu)}{k_B T}\right] \quad (1)$$

where P is the PA intensity, $h\nu$ is photon energy, k_B is the Boltzmann constant, T is absolute temperature, and P_0 , σ , E_0 are fitting parameters. σ is called steepness factor, which show a characteristic of exponential tail. By fitting Equation (1) to the PA spectra at the energy tail (1.8 eV - 2.0 eV) shown in **Figure 6**, σ can be determined. The values of σ for the IO-TiO₂/CdSe QD was found to decrease gradually from 0.23 to 0.20 as the post treatment cycles increase up to three cycles. Small σ means that disorders and/or impurities in the IO-TiO₂ electrodes increase. In other words, excess post treatment may result in disorders and impurities in the electrode.

Figure 7 shows the photocurrent density (J) versus photovoltage (V) characteristic of the four different IO-TiO₂/CdSe QDSSCs, where the IO-TiO₂ electrode was prepared with and without TiCl₄ post treatment. The values of J_{sc} , V_{oc} , FF, and η are shown in **Table 1**. Open circuit voltage (V_{oc}) is almost the same for all of the IO-TiO₂ electrodes (0.7 V), which is much higher than that of the CdSe QD sensitized nanoparticulate TiO₂ solar cells (0.5 V) [6]. In addition, short circuit current density (J_{sc}) was enhanced due to the amount of the adsorbed CdSe QDs increased after the TiCl₄ post treatment and has a maximum value of 6.33 mA/cm² at one cycle treatment, but decreased again for more than one cycle treatment, which results from excess TiCl₄ post treatment. This is because that the increase of surface area after the post treatment may lead to worse penetration of electrolyte. Therefore, there is an optimum cycle of the post treatment for

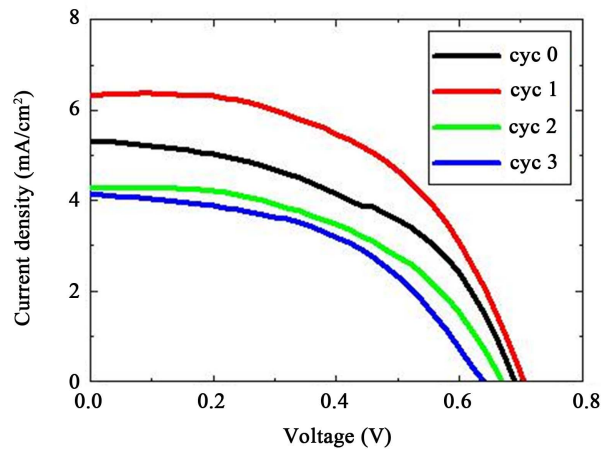


Figure 7. The photovoltaic properties of IO-TiO₂/CdSe QDSSCs, where the IO-TiO₂ was treated with and without TiCl₄ post treatment.

Table 1. Photovoltaic properties of different IO-TiO₂/CdSe QDSSCs, of which the IO-TiO₂ electrode was treated with and without TiCl₄ post treatment electrodes.

Cycle(s)	0	1	2	3
J _{sc} /mA·cm ⁻²	5.32	6.33	4.26	4.14
V _{oc} /V	0.69	0.71	0.67	0.64
Fill Factor	0.49	0.52	0.50	0.48
Efficiency/%	1.79	2.34	1.41	1.29

photovoltaic properties of the IO-TiO₂/CdSe QDSSCs. As a result, appropriate post treatment can improve the conversion efficiency of the solar cell.

Figure 8 shows the transient open circuit voltages of the IO-TiO₂/CdSe QDSSCs, of which the IO-TiO₂ electrode was treated with and without TiCl₄ post treatment electrodes. The electron lifetime in the QDSSCs can be calculated from the decay of V_{oc} (relative to carrier density) [14]. The electron lifetime can be determined by the following equation

$$\tau = \frac{k_B T}{e} \left(\frac{dV_{oc}}{dt} \right)^{-1} \quad (2)$$

where τ is the electron lifetime, k_B is the Boltzmann constant, T is absolute temperature, and e is elementary charge. The values of τ in each QDSSCs at 0.25 V are 1.5, 2.2, 0.2, 0.3 s corresponding to 0, 1, 2, 3 post treatment cycle(s) for the IO-TiO₂. This result indicates that the electron lifetime and recombination rate depend greatly on the post treatment cycle for IO-TiO₂. The longest electron lifetime for the QDSSCs with 1 cycle post treatment of the IO-TiO₂ is consistent with the best photovoltaic performance as shown in **Table 1** and **Figure 7**. This result indicates that the surface state of IO-TiO₂, is dependent strongly on the post treatment of the TiO₂ and control of the IO-TiO₂ properties by chemical treatment or surface passivation is very important for solar cell applications.

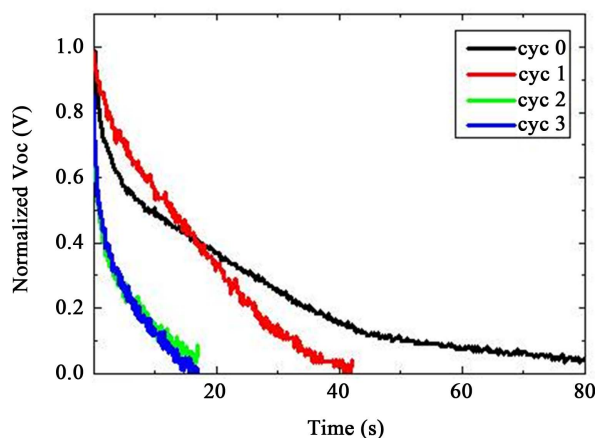


Figure 8. Transient open circuit voltages of different IO-TiO₂/CdSe QDSSCs, of which the IO-TiO₂ electrode was treated with and without TiCl₄ post treatment electrodes.

4. Conclusion

In summary, one of the most important factors in QDSSCs is the morphology and the property of the TiO₂ electrode. We applied TiCl₄ post treatment on IO-TiO₂ in order to increase surface area of IO-TiO₂, and investigated the effect of the post treatment on photovoltaic properties of CdSe QD sensitized IO-TiO₂ solar cells. In this case, the solar cell with one cycle post treated IO-TiO₂ showed the best photovoltaic properties because of large surface area and long electron lifetime, and this result indicates that excess post treatment may lead to both an increase in surface states and worse penetration of electrolyte. In order to search the method for improving the photovoltaic properties of QD sensitized inverse opal TiO₂ solar cells, it needs to control and optimize the charge separation interface further in the future.

Acknowledgements

This research was supported by the Japan Science and Technology Agency (JST) CREST program, the PRESTO program and the MEXT KAKENHI Grant (Grant Number 26286013).

References

- [1] Chiba, Y., Islam, A., Watanabe, Y., Komiya, R., Koide, N. and Han, L. (2006) *Japanese Journal of Applied Physics*, **45**, L638-L640.
<https://doi.org/10.1143/JJAP.45.L638>
- [2] Shen, Q., Arae, D. and Toyoda, T. (2004) *Journal of Photochemistry and Photobiology A: Chemistry*, **164**, 75-80.
- [3] Mora-Seró, I., Giménez, S., Fabregat-Santiago, F., Gómez, R., Shen, Q., Toyoda, T. and Bisquert, J. (2009) *Accounts of Chemical Research*, **42**, 1848-1857.
<https://doi.org/10.1021/ar900134d>
- [4] Toyoda, T., Onishi, Y., Katayama, K., Sawada, T., Hayase, S. and Shen, Q. (2013) *Journal of Materials Sciences and Engineering A*, **3**, 601-608.
- [5] Nozik, A. (2002) *Physica E*, **14**, 115-120.
- [6] Toyoda, T. and Shen, Q. (2012) *Journal of Physical Chemistry Letters*, **3**, 1885-1893.

- <https://doi.org/10.1021/jz3004602>
- [7] Diguna, L.J., Murakami, M., Sato, A., Kumagai, Y., Ishihara, T., Kobayashi, N., Shen, Q. and Toyoda, T. (2006) *Japanese Journal of Applied Physics*, **45**, 5563-5568. <https://doi.org/10.1143/JJAP.45.5563>
- [8] Zhang, X., Liu, Y., Lee, S., Yang, S. and Kang, Z. (2014) *Energy & Environmental Science*, **7**, 1409-1419. <https://doi.org/10.1039/c3ee43278e>
- [9] Shen, Q., Kobayashi, J., Diguna, L.J. and Toyoda, T. (2008) *Journal of Applied Physics*, **103**, Article ID: 084304.
- [10] Shen, Q., Yamada, A., Tamura, S. and Toyoda, T. (2010) *Applied Physics Letters*, **97**, Article ID: 123107.
- [11] Schroden, R.C., Daous, M.A., Blanford, C.F. and Stein, A. (2002) *Journal of Materials Chemistry*, **14**, 3305-3315. <https://doi.org/10.1021/cm020100z>
- [12] Brus, L.E. (1984) *Journal of Chemical Physics*, **80**, 4403-4409. <https://doi.org/10.1063/1.447218>
- [13] Urbach, F. (1953) *Physical Review*, **92**, 1324. <https://doi.org/10.1103/PhysRev.92.1324>
- [14] Zaban, A., Greenshtein, M. and Bisquert, J. (2003) *Chemphyschem Communications*, **4**, 859-864. <https://doi.org/10.1002/cphc.200200615>



Submit or recommend next manuscript to SCIRP and we will provide best service for you:

Accepting pre-submission inquiries through Email, Facebook, LinkedIn, Twitter, etc.
A wide selection of journals (inclusive of 9 subjects, more than 200 journals)
Providing 24-hour high-quality service
User-friendly online submission system
Fair and swift peer-review system
Efficient typesetting and proofreading procedure
Display of the result of downloads and visits, as well as the number of cited articles
Maximum dissemination of your research work

Submit your manuscript at: <http://papersubmission.scirp.org/>

Or contact jmp@scirp.org